Supplementary Information

Controlling ZIF-67 film properties in water-based cathodic electrochemical deposition

Eman Elsayed[1,*], Ignacio Brevis [2], Sathish Pandiyan[3], Ricky Wildman[3], Kristoffer G. van der Zee[2], Begum Tokay[1,*]

[1]Department of Chemical and Environmental Engineering, Faculty of Engineering, University of Nottingham, University Park, NG7 2RD, UK.
[2]Centre for Additive Manufacturing, Faculty of Engineering, University of Nottingham, Nottingham, NG7 2RD, UK.
[3]School of Mathematical Sciences, University of Nottingham, Nottingham, NG7 2RD, UK.

* Corresponding authors e-mail: eng.eman.m.elsayed@gmail.com; eman.hussein@nottingham.ac.uk, begum.tokay@nottingham.ac.uk

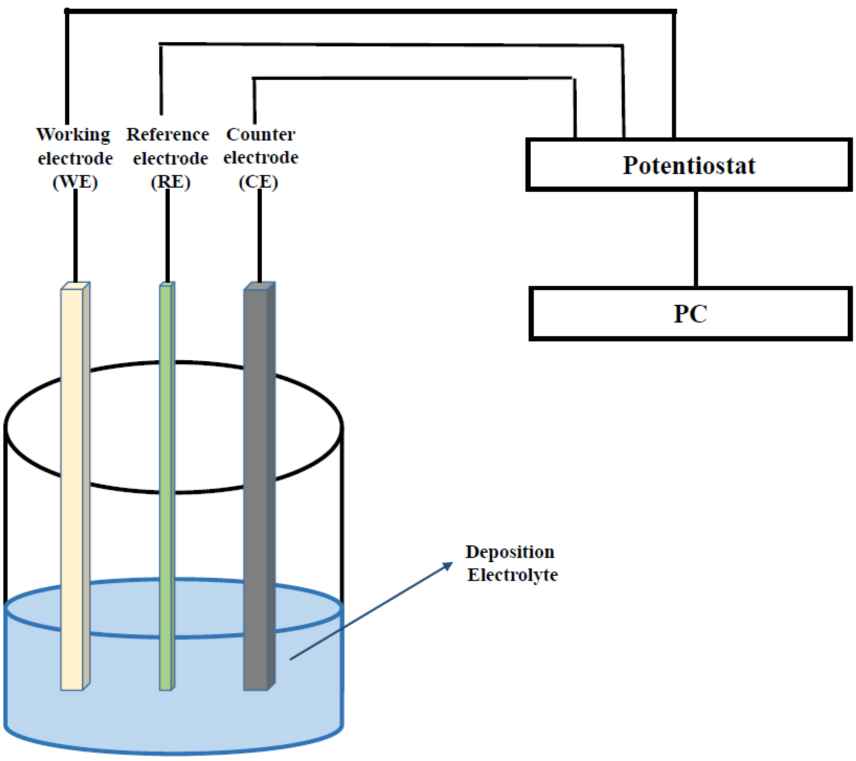

Fig. S1 Three-electrode electrochemical cell for the fabrication of ZIF-67 film on ITO/PET substrate.
(Working electrode (WE): ITO/PET substrtate, Reference electrode (RE): Ag/AgCl and Counter electrode (CE): platinum wire)
(Electrolyte solution: 10 ml 0.099 M $Co(NO_3)_2{\cdot}6H_2O$ and 40 ml 1.75 M HMim)

Table S1 Volumes of HNO_3 and NaOH used to adjust solution pH.

pH	Volume of HNO_3(ml)	Volume of NaOH(ml)
7	2.7	-
8	1.6	-
9	0.8	-
11.6		0.075
12.5		0.11

Table S2 Matrix developed for investigated molar ratio of ZIF-67 solution reactants.

Linker/metal molar ratio	Concentration (M)	Conductivity (μS/cm)	pH
1	**HMim: 1.75**	34,720±140	7.17±0.07
4		10,300±7.07	8.79±0.13
6		7,718±2.83	9.15±0.01
8.83		5,430±0.71	9.28±0.07
16		3,285±0.71	9.57±0.07
25		2,106±1.41	9.76±0.07
35.34		1,582±0.71	9.85±0.07
70.68		903.5±0.71	10.11±0.07
1	**$Co(NO_3)_2$: 0.099**	3,323±8.49	8.39±0.07
4		3,072±2.83	9.13±0.07
6		2,952±17.7	9.33±0.07
8.83		2,918±7.07	9.36±0.07
16		2667±2.33	9.73±0.07
25		2315±11.3	9.94±0.07
35.34		1947±1.41	10.05±0.07
70.68	Over the solubility limit of HMim in water		

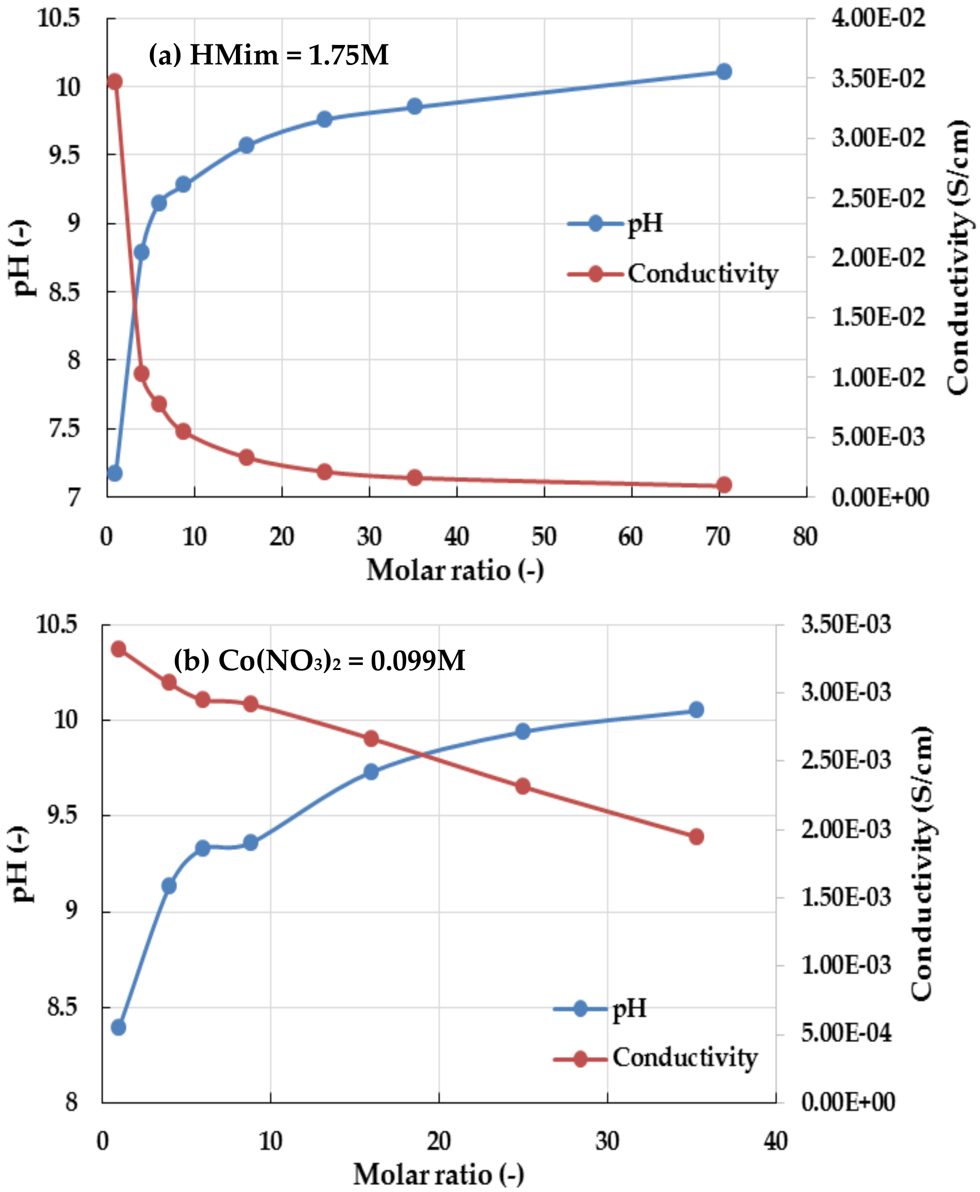

Fig. S2 Effect of molar ratio on the reaction solution pH and conductivity at fixed a. HMim concentration= 1.75 M and b. Co nitrate concentration= 0.099 M.

1.1. Statistical analysis

Standard deviations were calculated and included with all data presented in the current study. Also, as correlation coefficients describing the strength and direction of an association between variables, Pearson and Spearman correlations along with their associated p-values were calculated. Pearson and Spearman correlations are considered as the most frequently used correlation indices. The first one measures the linear relationship between two continuous random variables and is adopted when the data follows a normal distribution while the second one measures any monotonic relationship between two continuous random variables and is adopted when the data do not follow a normal distribution; both range from -1 to 1 [1].

The Pearson correlation can be calculated through:

$$r = \frac{\sum(x_i - \bar{x})(y_i - \bar{y})}{\sqrt{\sum(x_i - \bar{x})^2 \sum(y_i - \bar{y})^2}} \qquad \textbf{Eq. 1}$$

Where:

r is the Pearson's correlation coefficient, x_i is value of x in a sample, $\bar{x}$ is the mean value of x, y_i is value of y in a sample and $\bar{y}$ is the mean value of y.

The Spearman correlation can be calculated through:

$$\rho = 1 - \frac{6\sum d_i^2}{n(n^2-1)} \qquad \textbf{Eq. 2}$$

Where:

ρ is the Spearman's correlation coefficient, d is difference between the two ranks of each observation and n is number of observations.

The p-value for the data sets was then calculated through:

$$\text{p-value} = P(T|H_0) \qquad \textbf{Eq. 3}$$

where:

P is probability, T is testing results indicating the null hypothesis is not true, | given that and H_0 null hypothesis is true.

The P stands for probability and indicates how probable it is that any observed variation between groups is the result of chance. As a probability, P can have any value between 0 and 1. Values near to zero (less than 0.05) imply that the observed difference is unlikely to be attributable to chance (statistically significant), whereas a P value close to one indicates that there is no difference between the groups other than by chance [2].

The relation between different variables such as applied potential, molar ratio, crystal size and surface coverage were fitted to obtain mathematical expressions using Engineering Equation Solver (EES) software.

Fig. S3 shows a plot of the effect of molar ratio (fixed Cobalt nitrate concentration) on the measured solution pH and conductivity. It can be noticed that the relation between the molar ratio and conductivity is perfectly linear while it is not in case of pH, hence Pearson's correlation coefficient was calculated for the former while Spearman's correlation coefficient was calculated for the latter.

Fig. S4 shows a plot of the effect of molar ratio (fixed HMim concentration) on the measured solution pH and conductivity. It can be noticed that the relation between all the variables is non-linear, hence Spearman's correlation coefficient was calculated.

Values of Spearman's correlation coefficients are shown in **Table S3** in which a very small p-value was calculated.

Such significantly low p-values is statistically significant which means that there negligible probability that the relationship between molar ratio of reactants, solution conductivity and solution pH might have happened by chance and there is a strong relation between the variables.

Proposed mathematical expression to fit the relation between molar ratio (constant cobalt nitrate concentration) and solution conductivity (**Eq. 4**) and molar ratio (constant cobalt nitrate concentration) and solution pH (**Eq. 5**).

$$Y = 3257.467 - 37.512X \qquad \textbf{Eq. 4}$$

$$Z = 8.431 + 0.463LN(X) \qquad \textbf{Eq. 5}$$

The relation between molar ratio (constant HMim concentration) and solution conductivity and pH is shown in **Eq. 6** and **7**.

$$Y = 34935.926X^{-0.862} \qquad \textbf{Eq. 6}$$

$$Z = 7.651 + 0.65LN(X) \qquad \textbf{Eq. 7}$$

Where Y is solution conductivity, X is molar ratio and Z is the solution pH. The fitting of the experimental data is shown in **Fig. S5** and **S6** where good agreement between the experimental data and proposed expressions can be observed.

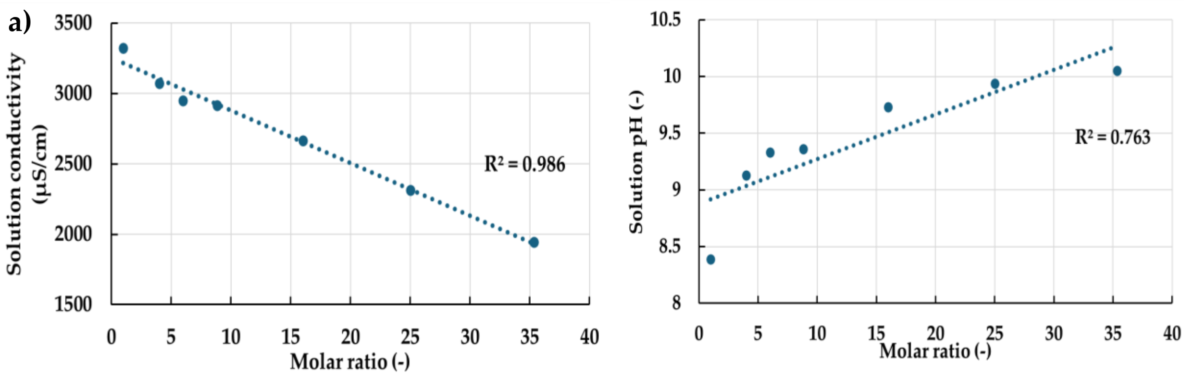

Fig. S3 Linear fitting of molar ratio (fixed Cobalt nitrate) with a. conductivity and b. pH of ZIF-67 reaction solution.

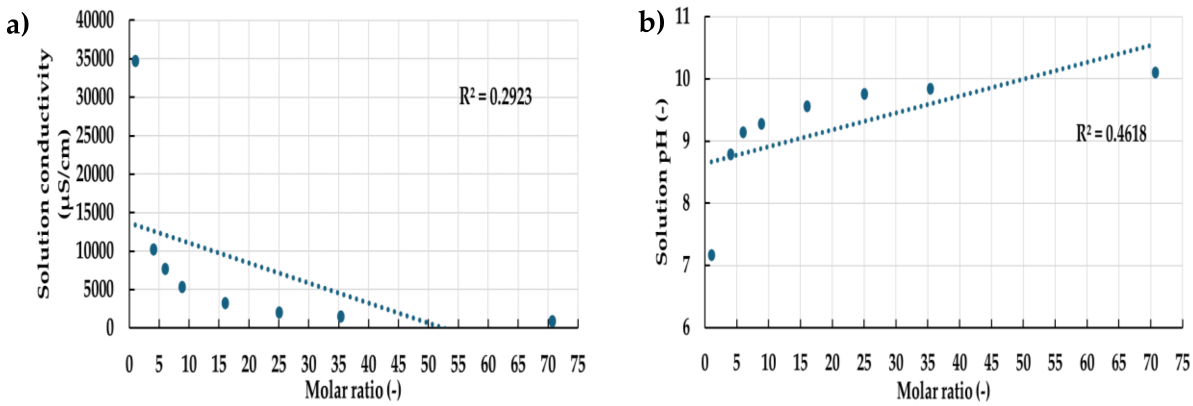

Fig. S4 Linear fitting of molar ratio (fixed HMim) and a. conductivity and b. pH of ZIF-67 reaction solution.

Table S3 Spearman/Pearson correlation coefficients and p-value for relation between molar ratio, solution conductivity and solution pH.

Fixed cobalt nitrate		
	Molar ratio-conductivity	Molar ratio-pH
Spearman's rank/Pearson's correlation coefficient	-0.993	1
P-value	7.8E-06	1.9E-05
Fixed HMim		
Spearman's rank/Pearson's correlation coefficient	-1	1
P-value	2.5E-06	2.5E-06

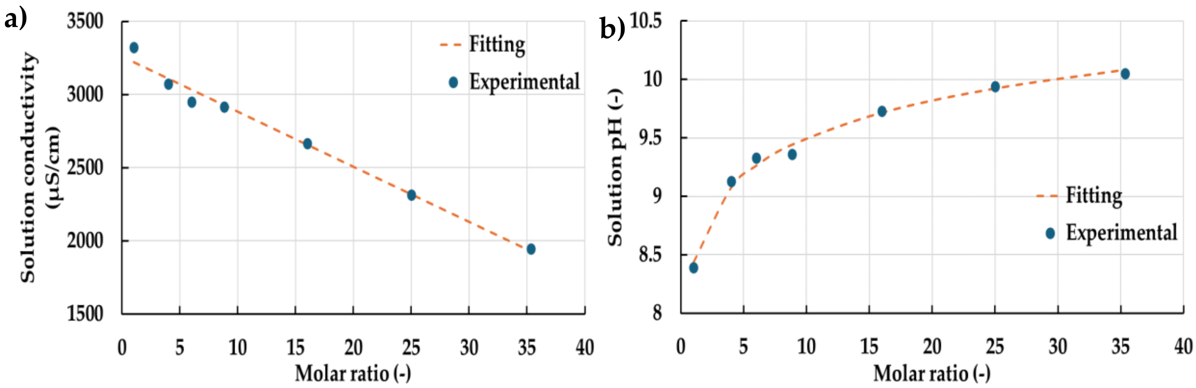

Fig. S5 Proposed fitting of molar ratio (fixed Cobalt nitrate) relation with a. conductivity and b. pH of ZIF-67 reaction solution.

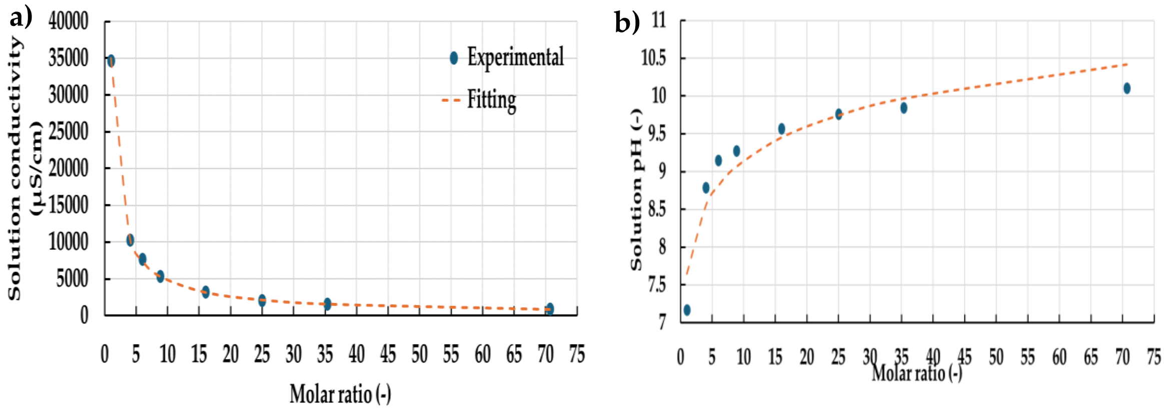

Fig. S6 Proposed fitting of molar ratio (fixed HMim) relation with a. conductivity and b. pH of ZIF-67 reaction solution.

Table S4 Volumes of HNO_3 and NaOH used to adjust solution pH of molar ration=1 (MR1) and molar ration=16 (MR16).

MR	pH before adjustment	pH after adjustment	Volume of HNO_3(ml)	Volume of NaOH(ml)
1	8.39	12	-	0.2
16	9.73	8	1.1	-

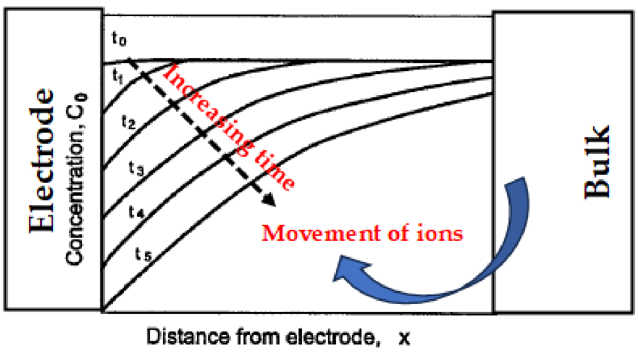

Fig.S7 Variation of concentration of reactant during non-steady-state electrolysis.

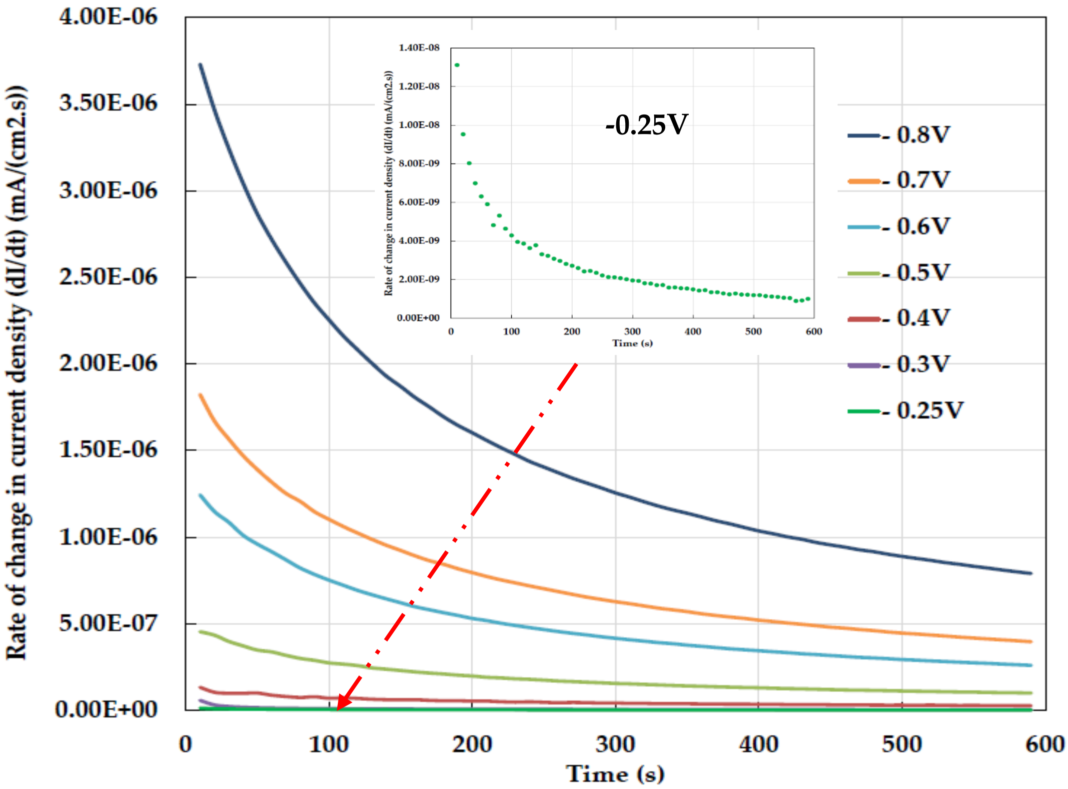

Fig. S8 Effect of applied potential on the change rate in current density (dI/dt)

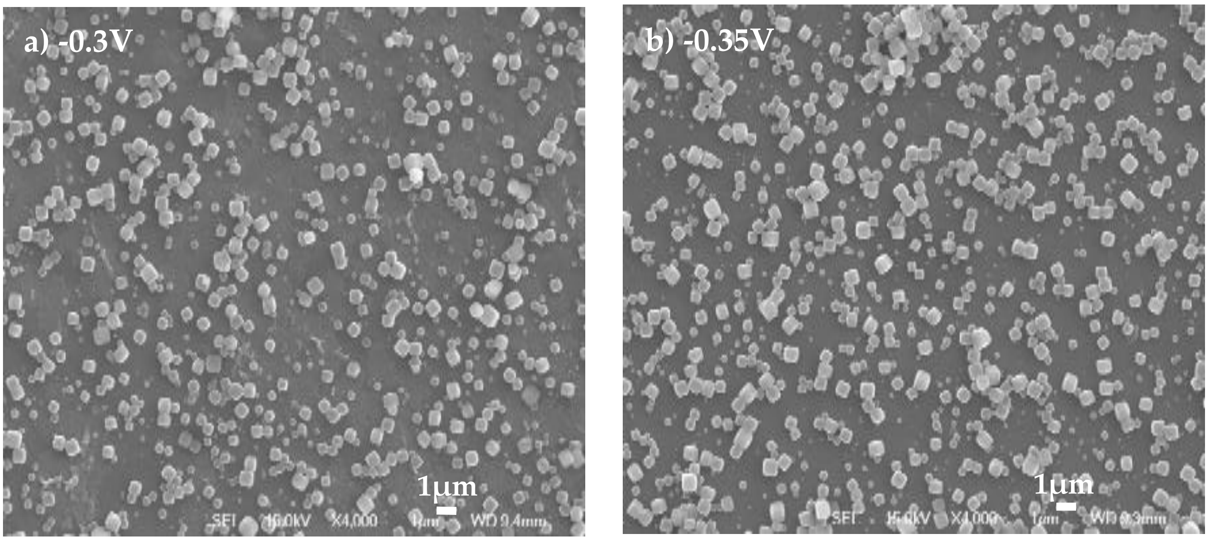

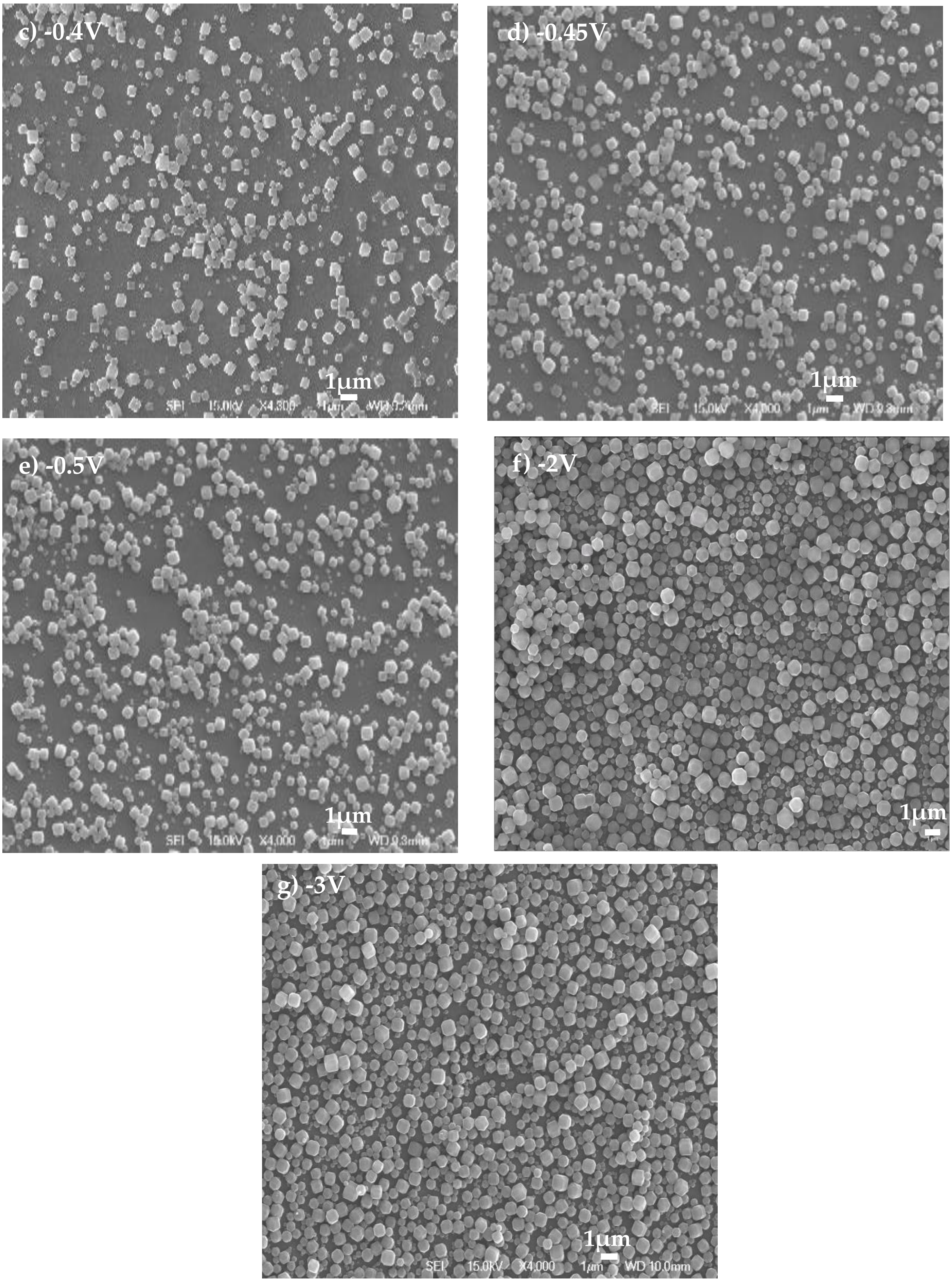

Fig. S9 SEM images of ZIF-67 films at potentials a. -0.3V, b. -0.35V, c. -0.4V, d. -0.45V, e. -0.5V, f. -2V and g. -3V for 10 min.

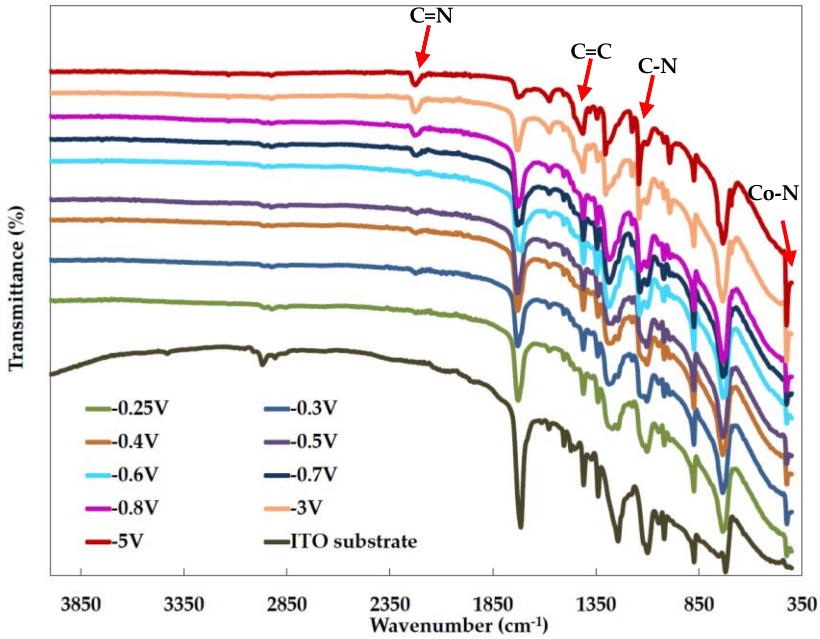

Fig. S10 FTIR spectrum of formed ZIF-67 film at applied potentials between -0.25 to-5 V for 10 min.

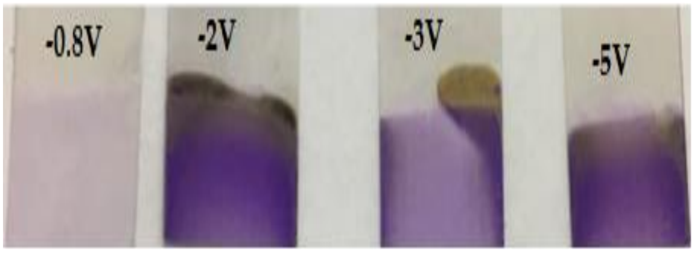

Fig. S11 Images of formed ZIF-67 films and substrates at different potentials higher than -0.8V for 10 min.

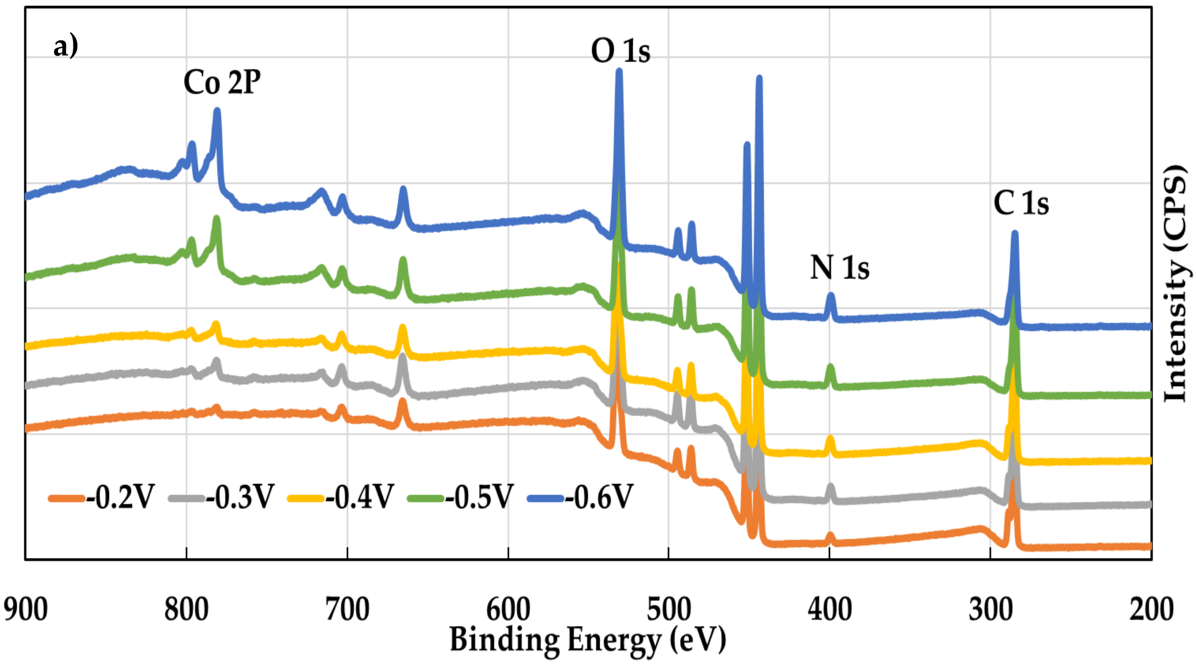

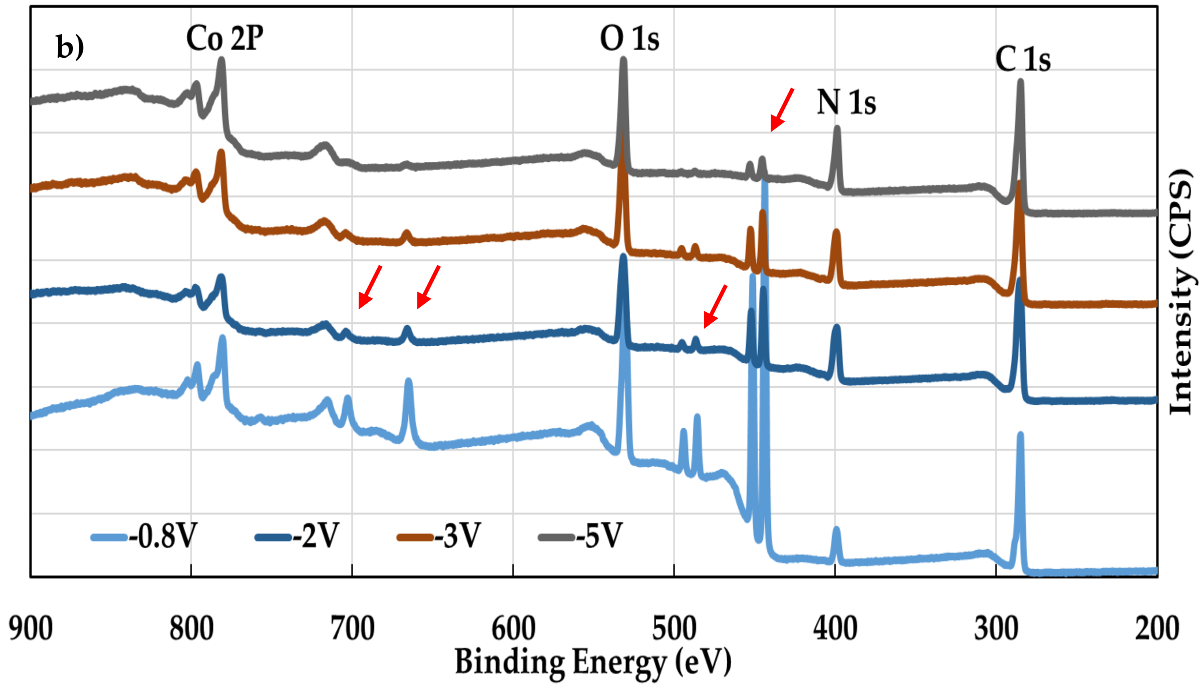

Fig. S12 Wide scan XPS survey spectra of electrodeposited ZIF-67 film developed at different applied potentials (a. -0.2V to -0.6V and b. -0.8V to -5V) for 10 min. (Red arrows to highlight the Sn and In peaks from conductive ITO)

Fig. S13 shows a plot of the effect of applied potential on the surface coverage and crystal size of electrodeposited ZIF-67. It can be noticed that the relation between the variables is not perfectly linear, hence Spearman's correlation coefficient was calculated. Values of Spearman's correlation coefficients are shown in **Table S5** in which a significantly low p-value was calculated.

Such low p-values is statistically significant which means that there is a negligible probability that the relationship between applied potential, surface coverage and crystal size of electrodeposited ZIF-67 might have happened by chance.

Proposed mathematical expression to fit the relation between applied potential and crystal size (**Eq. 8**) and applied potential and surface coverage (**Eq. 9**).

$Y=0.683+ 0.981X+ 0.623X^2$ **Eq. 8**

$Z=-79.673 - 666.585X - 1289.79X^2 - 814.517X^3$ **Eq. 9**

Where Y is crystal size (μm), X is applied pressure (V) and Z is the surface coverage (%). The fitting of the experimental data is shown in **Fig. S14** where good agreement between the experimental data and proposed expressions can be observed.

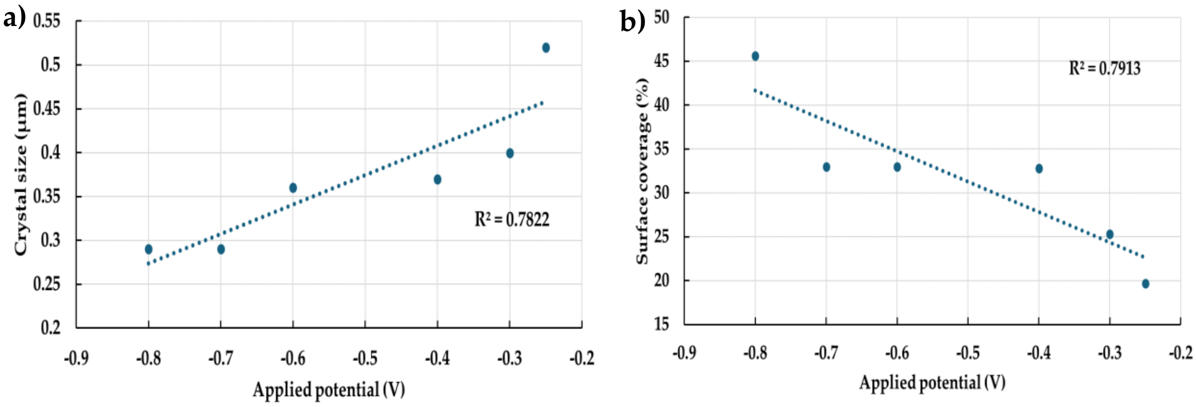
a)
Crystal size (µm)
0.55
0.5
0.45
0.4
0.35
0.3
0.25
0.2
R² = 0.7822
-0.9
-0.8
-0.7
-0.6
-0.5
-0.4
-0.3
-0.2
Applied potential (V)
b)
Surface coverage (%)
50
45
40
35
30
25
20
15
R² = 0.7913
-0.9
-0.8
-0.7
-0.6
-0.5
-0.4
-0.3
-0.2
Applied potential (V)

Fig. S13 Linear fitting of applied potential with a. crystal size and b. surface coverage of electrodeposited ZIF-67 film.

Table S5 Spearman correlation coefficient and p-value for relation between applied potential, crystal size and surface coverage.

	Applied potential-Crystal size	Applied potential-Surface area
Absolute Spearman's rank correlation coefficient	0.98	0.98
P-value	3.1E04	3.1E04

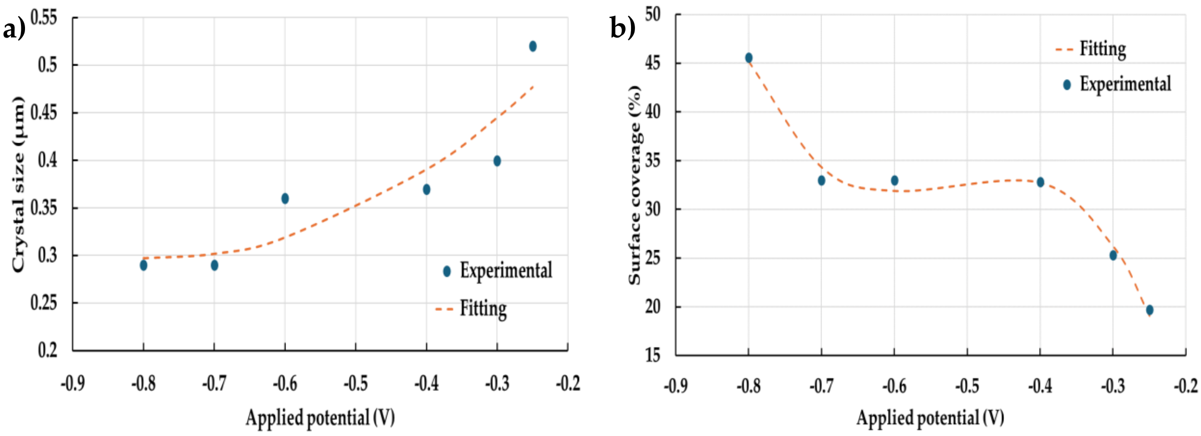

Fig. S14 Proposed fitting of applied potential with a. crystal size and b. surface coverage of electrodeposited ZIF-67 film.

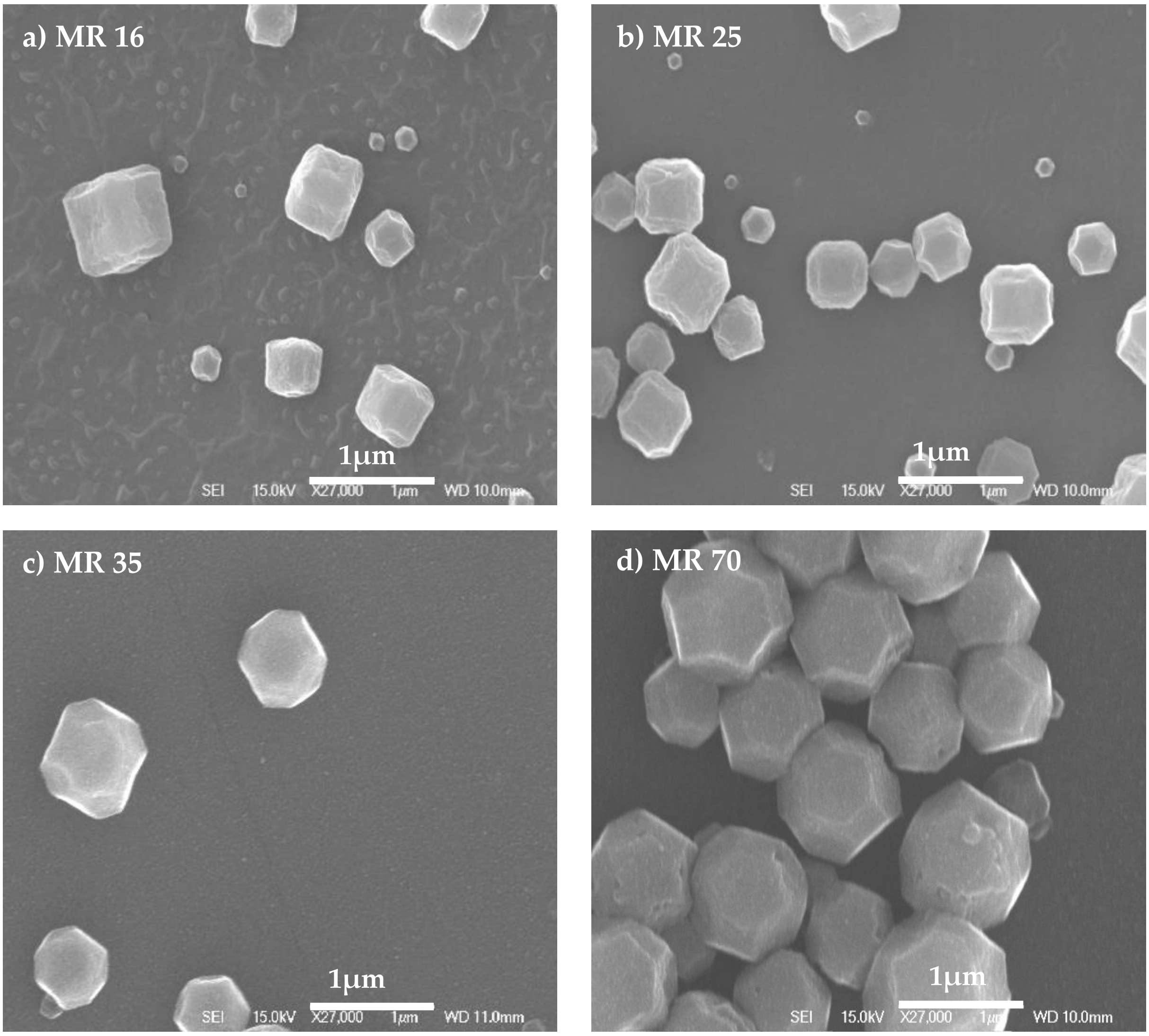

Fig. S15 SEM images of ZIF-67 films at different molar ratio between 16-70 a. MR 16, b. MR 25, c. MR 35 and d. MR 70 (HMim concentration= 1.75 M) at -0.8V for 10 min.

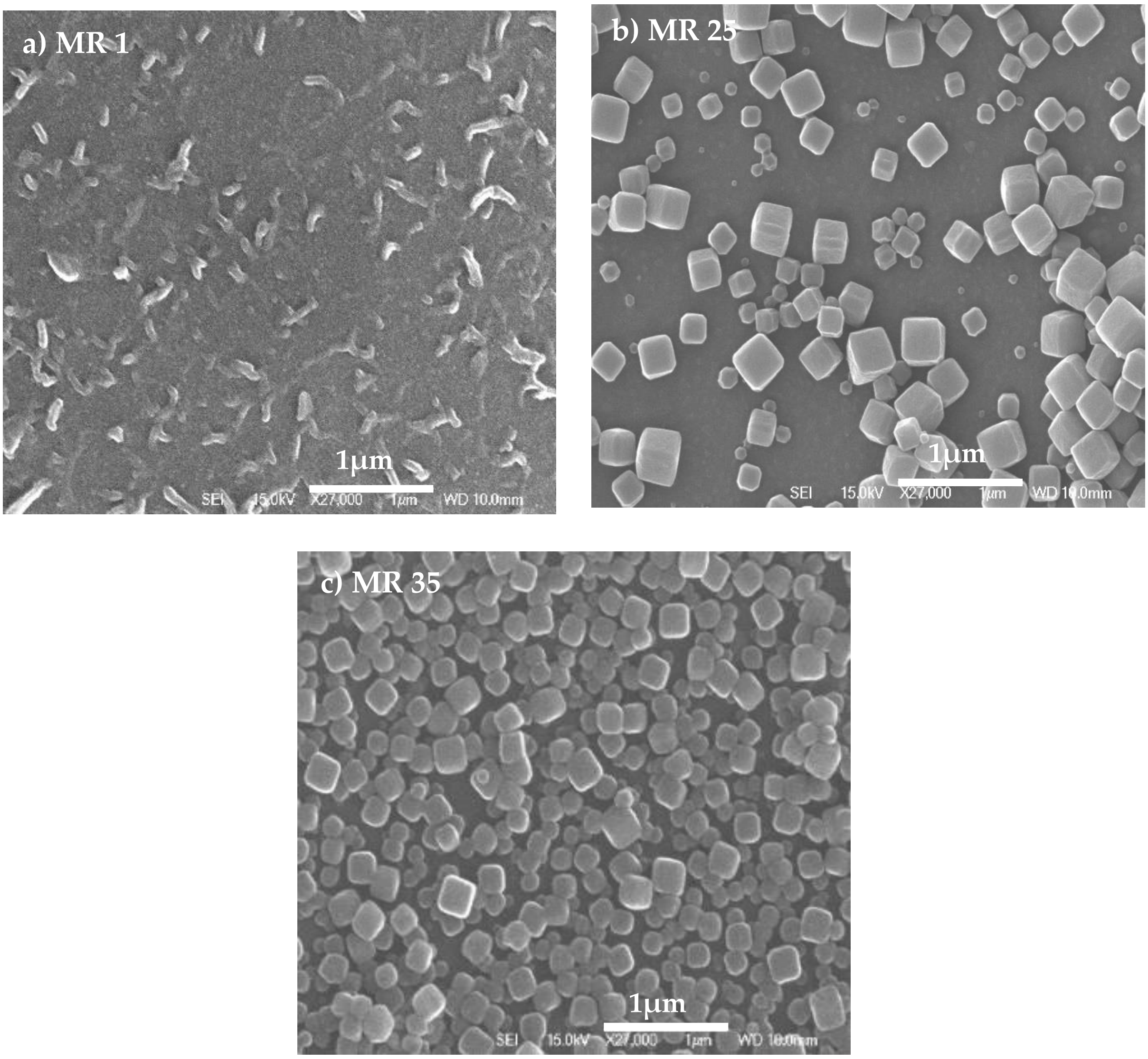

Fig. S16 SEM images of ZIF-67 films at different molar ratios a. MR 1, b. MR 25 and c. MR 35 (cobalt nitrate concentration= 0.099 M) at -0.8V for 10 min.

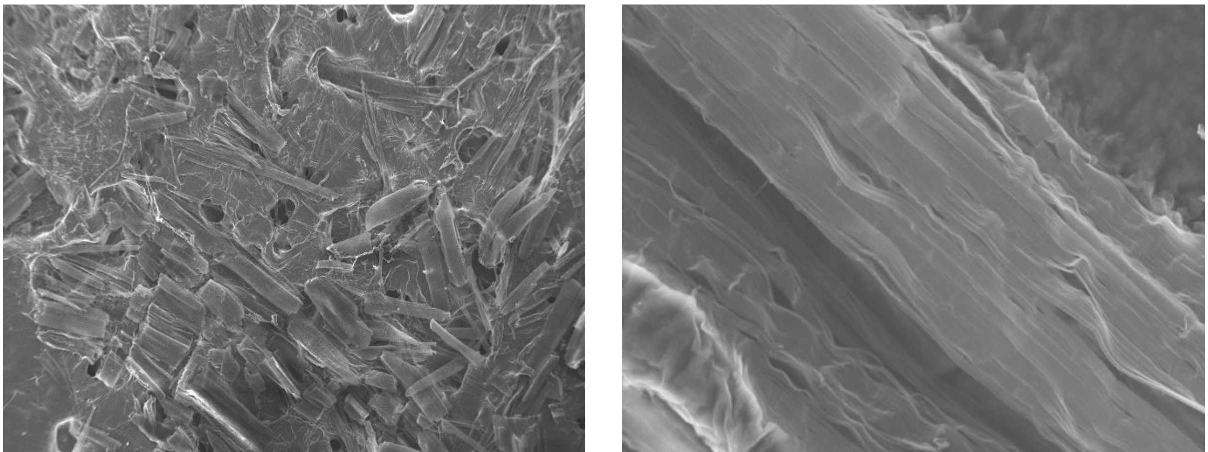

Fig S17 SEM images of HMim.

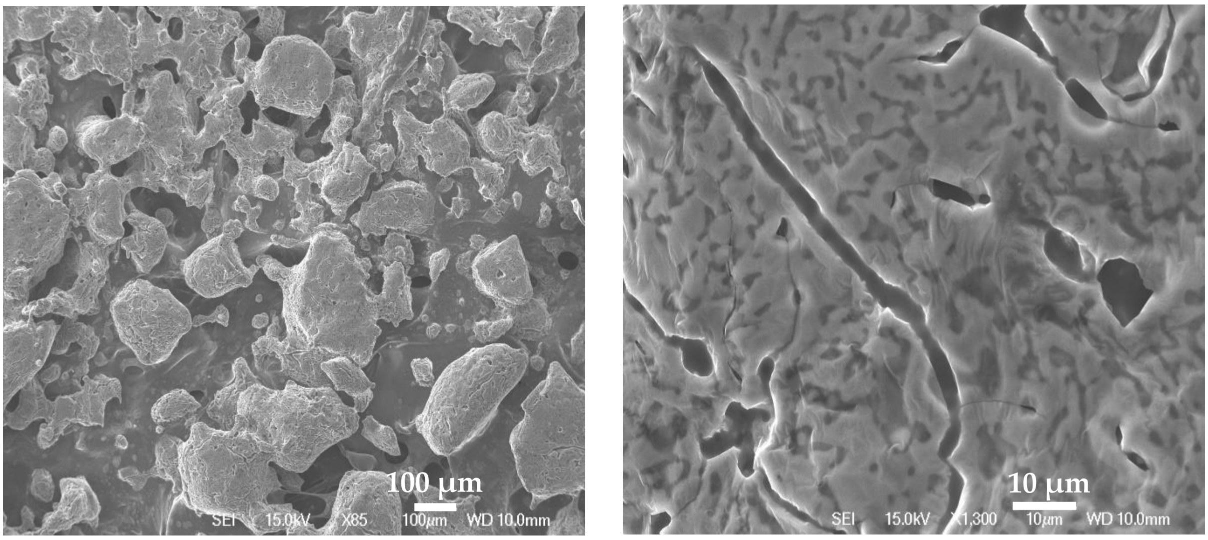

Fig. S18 SEM images of Cobalt nitrate hexahydrate.

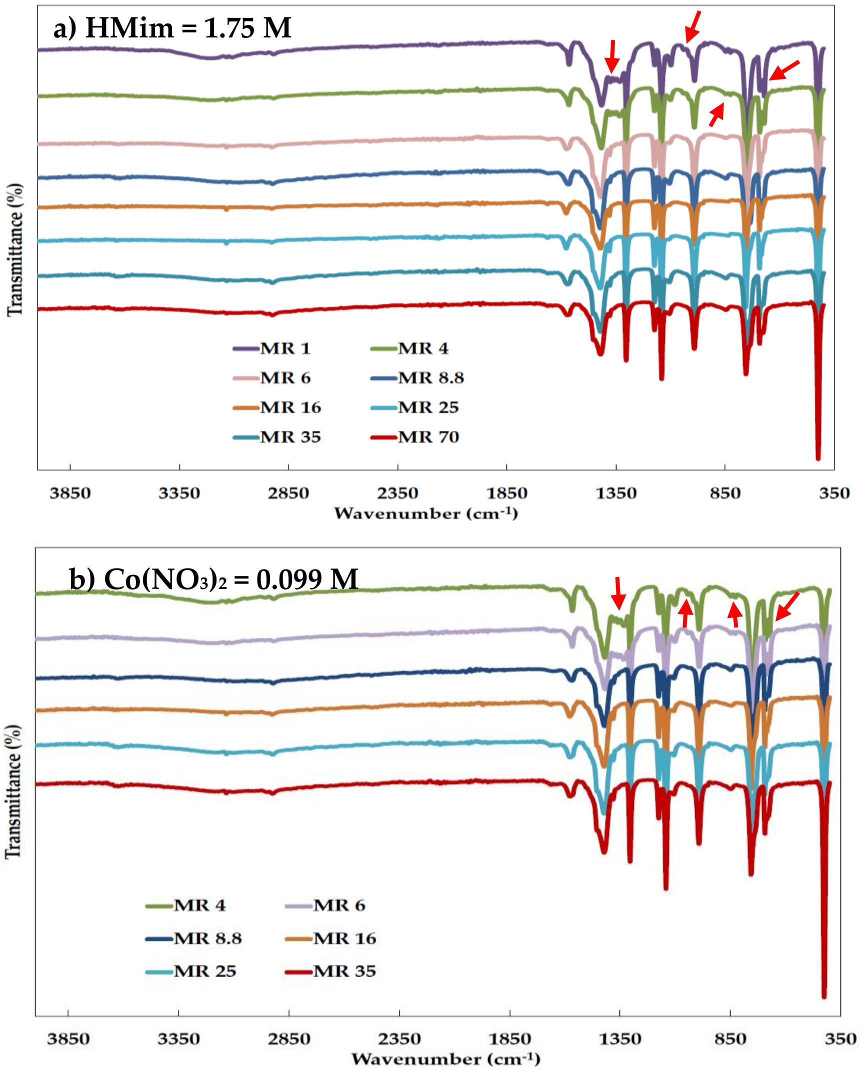

Fig. S19 FTIR spectrum of formed ZIF-67 powders at different molar ratios at fixed a. HMim and b. cobalt nitrate concentrations at -0.8V for 10 min.

Fig. S20 shows the wide scan and high-resolution scans of Co, N, C and O of the ZIF-67 developed using a reaction solution with a MR 8.8 at -0.8 V for 10 min (HMim concentration= 1.75 M). The high-resolution XPS spectrum for C 1s was attributed to peaks corresponding to binding energies (BE) of carbon in a functional group such as to sp2-C, C–N, N-C=O, C=O and carboxyl groups (O=C–O) [3, 4]. The fitted N 1s spectra was attributed to 4 peaks corresponding to binding energies (BE) of nitrogen in a functional group such as, nitrite, quaternary nitrogen, Co–N, and pyrrolic nitrogen, respectively. The formation of the Co–N bond is characteristic feature for the formation of ZIF-67 as indicated from FTIR spectrum. The XPS spectrum of Co $2p_{3/2}$ was segmented into 4 peaks, representative of Co^{3+}, CoO, Co–Nx, and satellite. Thus, the XPS result confirms the coexistence of cobalt and nitrogen bond in the well-structured ZIF-67. The O 1s can be deconvoluted into 4 peaks corresponding to be adsorbed O, C-OH (hydroxyl), C-O-C (epoxy), and carbonate structures.

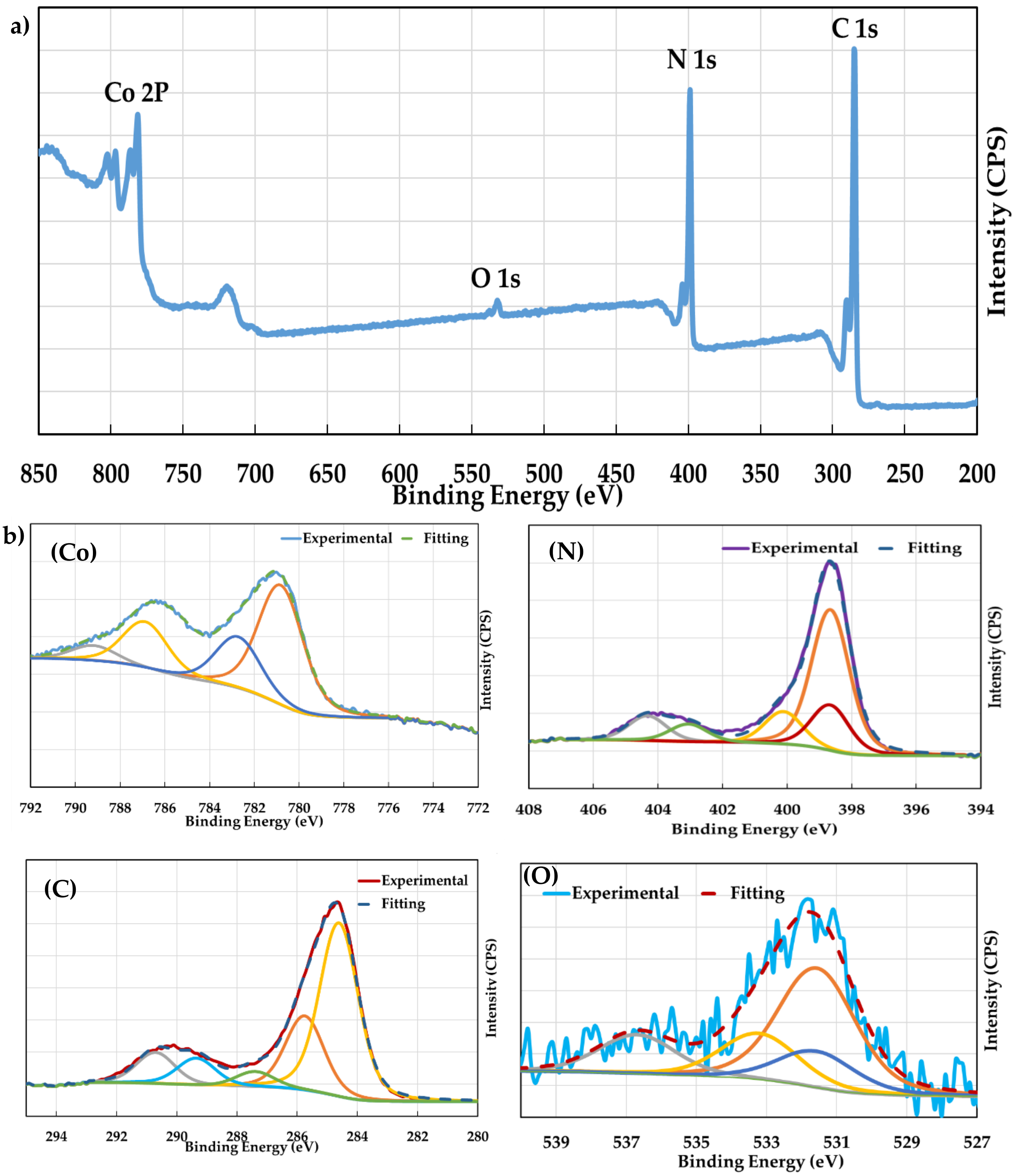

Fig. S20 XPS survey spectrum (a. wide scan and d. high-resolution scans of Co, N, C and O) of ZIF-67 powder collected at -0.8 V for 10 min for MR 8.8 (HMim concentration= 1.75 M).

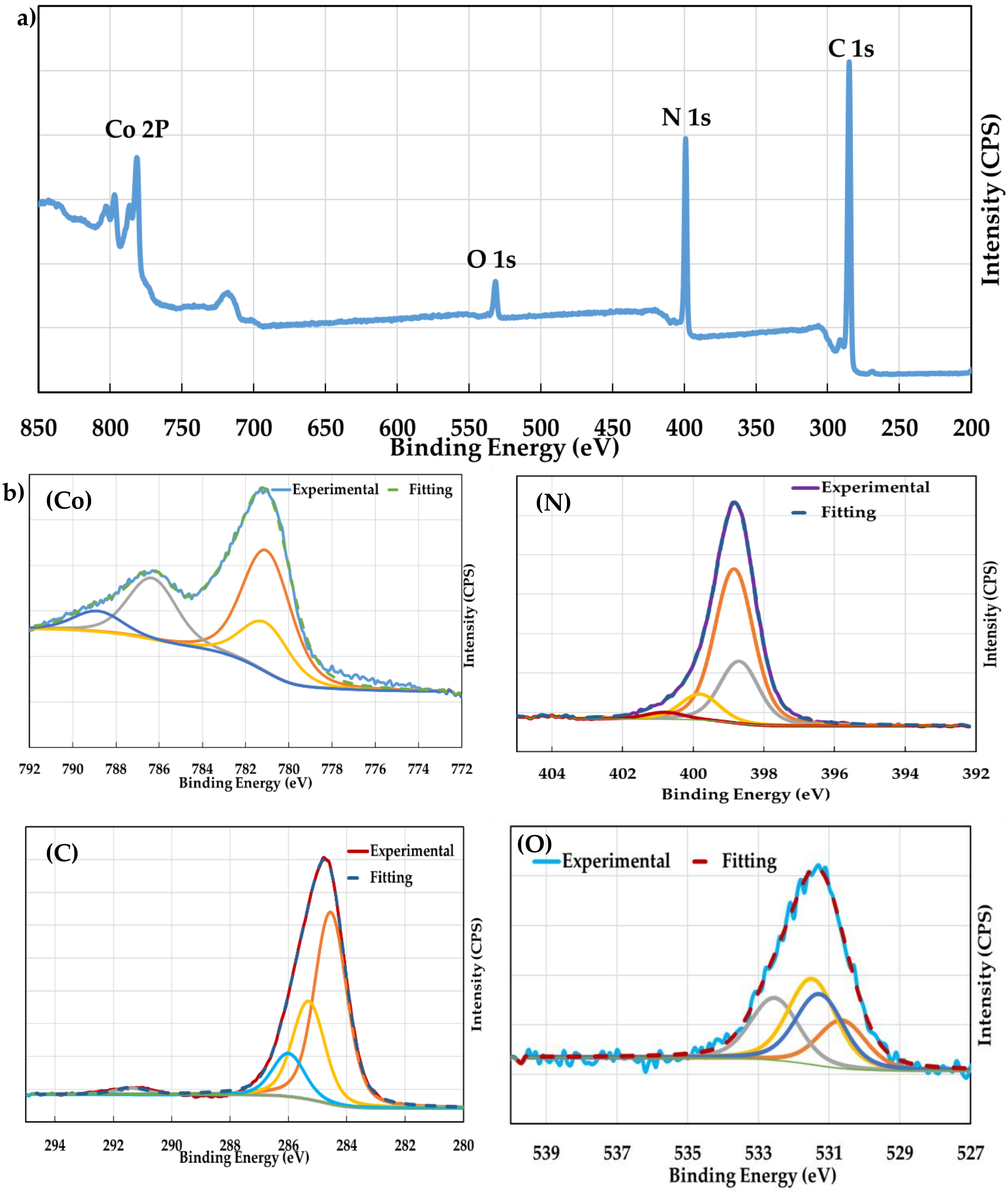

Fig. S21 XPS survey spectrum (a. wide scan and d. high-resolution scans of Co, N, C and O) of ZIF-67 powder collected at -0.8 V for 10 min for MR 8.8 (cobalt nitrate concentration= 0.099 M).

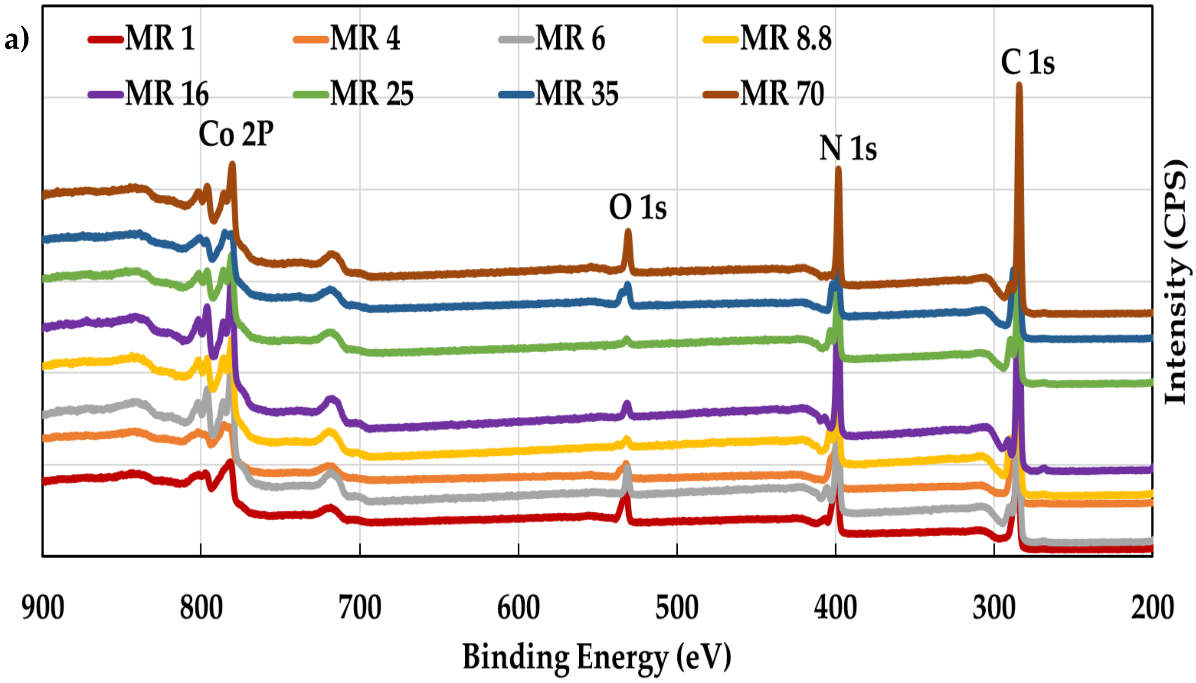

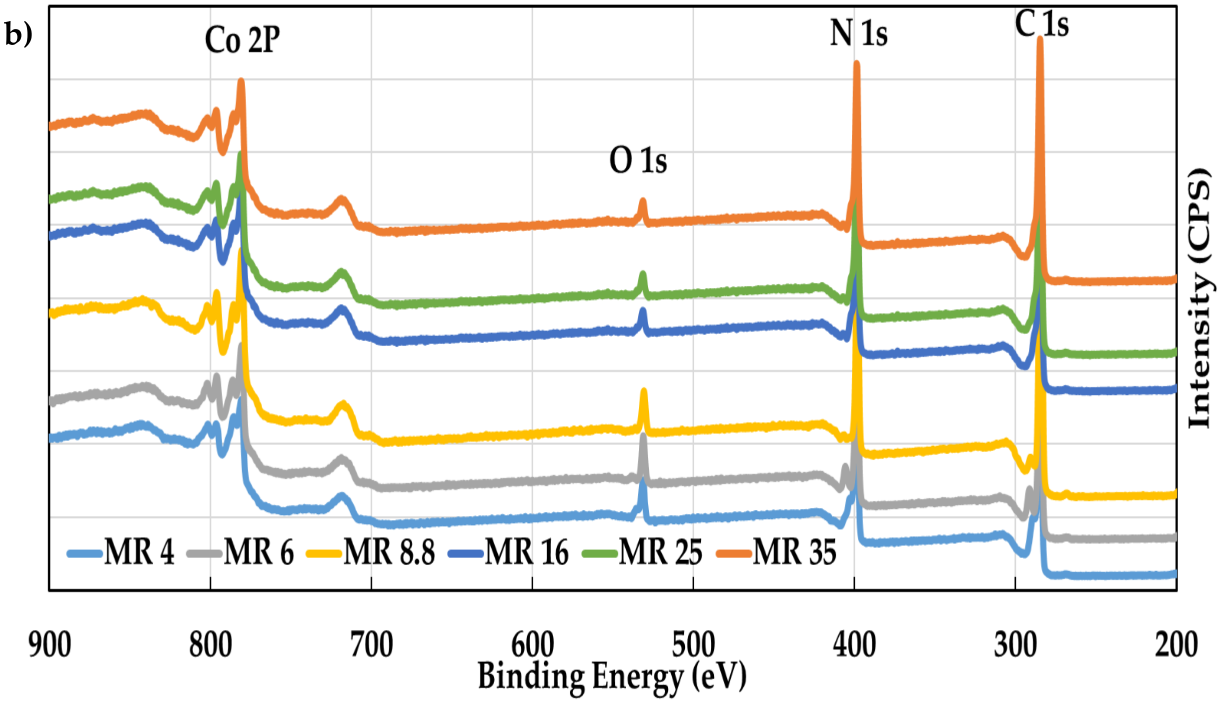

Fig. S22 Wide scan XPS survey spectra of ZIF-67 powders collected at different molar ratios (a. HMim concentration= 1.75 M and b. cobalt nitrate concentration= 0.099 M) at -0.8V for 10 min.

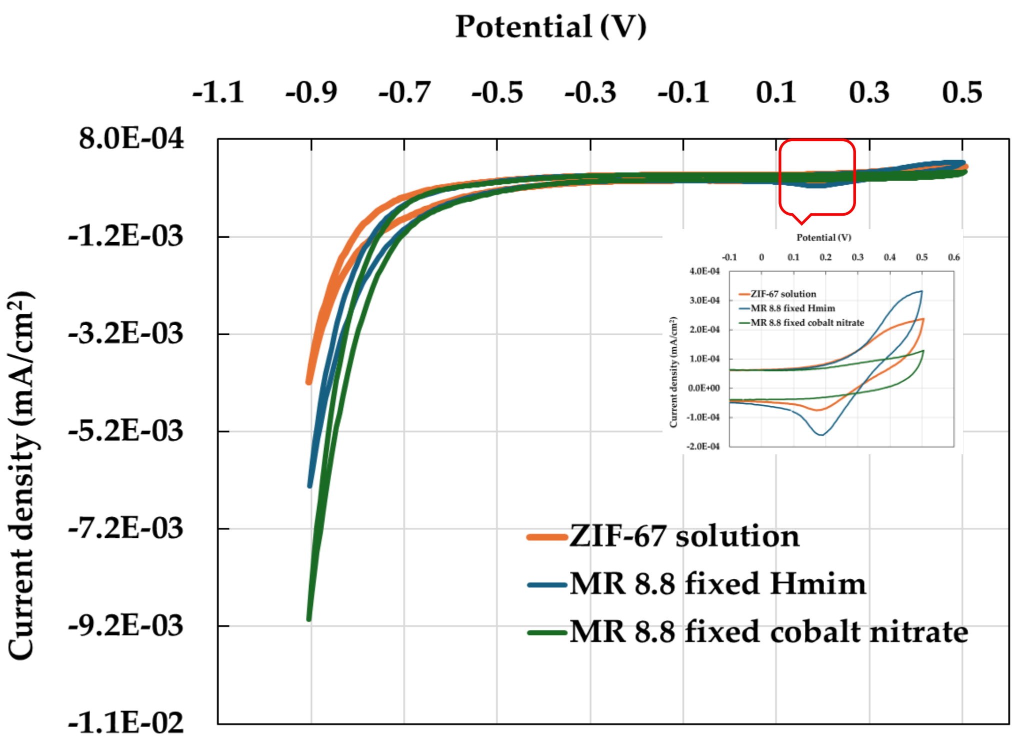

Fig. S23 Cyclic Voltammetry of ZIF-67 solutions on ITO/PET substrate.

Fig. S24 shows a plot of the effect of molar ratio (fixed HMim concentration) on the surface coverage and crystal size of electrodeposited ZIF-67. It can be noticed that the relation between the molar ratio and crystal size is perfectly linear while it is not in case of surface coverage, hence Pearson's correlation coefficient was calculated for the former while Spearman's correlation coefficient was calculated for the latter. Values of Spearman's and Pearson's correlation coefficients are shown in **Table S6**.

Such significantly low p-values is statistically significant which means that there is a negligible probability that the relationship between molar ratio of reactants, surface coverage and crystal size might have happened by chance and there is a strong relation between the variables.

Proposed mathematical expression to fit the relation between molar ratio (constant HMim concentration) and surface coverage (**Eq. 10**) and crystal size (**Eq. 11**).

$Y = 31.943 - 0.742X + 0.006X^2$ **Eq. 10**

$Z = 0.276 + 0.007X$ **Eq. 11**

Where Y is surface coverage, X is molar ratio and Z is the crystal size. The fitting of the experimental data is shown in **Fig. S25** where good agreement between the experimental data and proposed expressions can be observed.

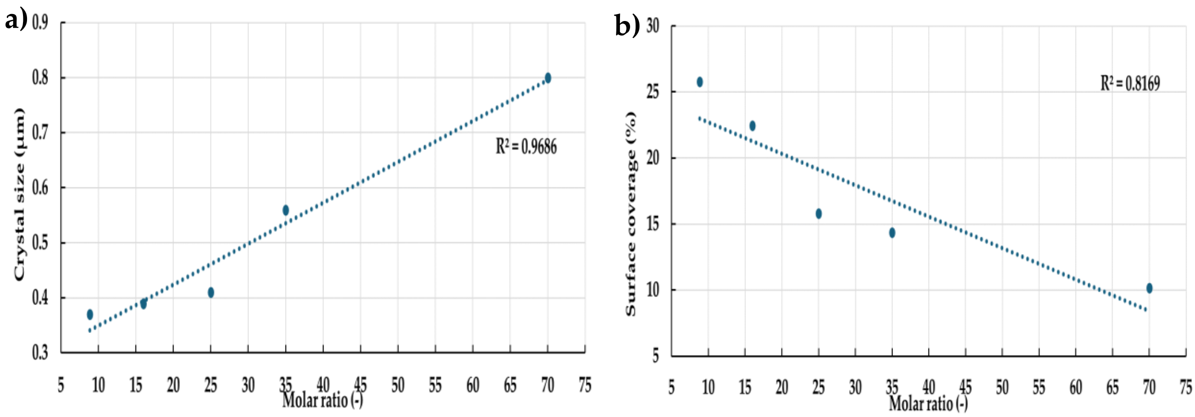

Fig. S24 Linear fitting of molar ratio (fixed HMim) with a. crystal size and b. surface coverage of electrodeposited ZIF-67 films.

Table S6 Spearman correlation coefficient and p-value for relation between molar ratio (fixed HMim concentration), crystal size and surface coverage.

	Molar ratio-Crystal size	Molar ratio-Surface area
Spearman's rank correlation coefficient	0.98	-1
P-value	2.38E-03	1.20E-03

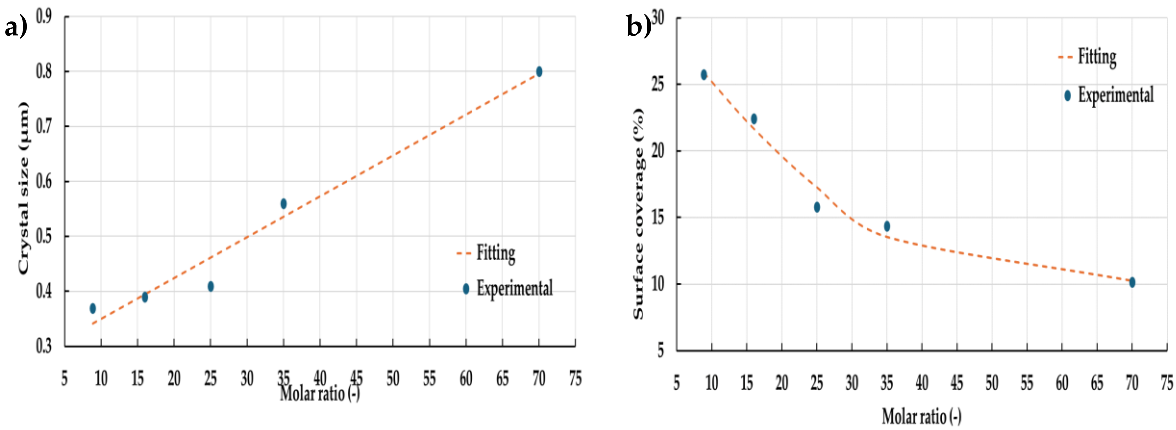

Fig. S25 Proposed fitting of molar ratio (fixed HMim) with a. crystal size and b. surface coverage of electrodeposited ZIF-67 films.

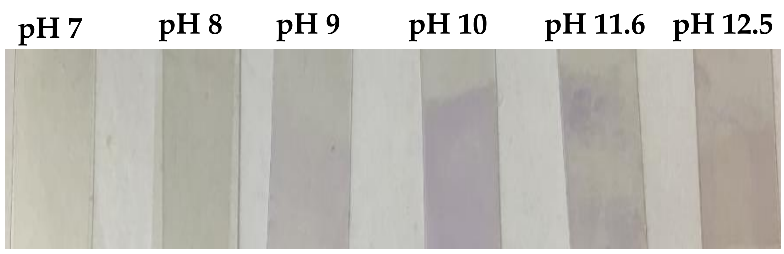

Fig. S26 Electrodeposited ZIF-67 films at -0.8 V for 10 min at various solution pH values.

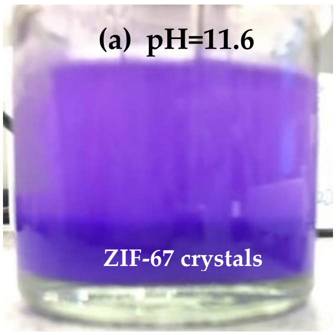

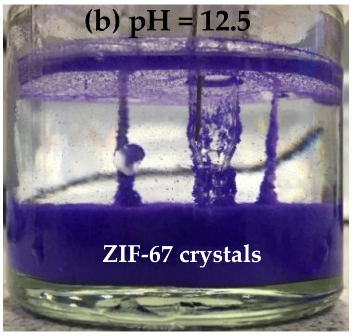

Fig. S27 Separation of ZIF-67 crystals from reaction solution for 10 min at -0.8 V at solution pH of a. 11.6 and b. 12.5.

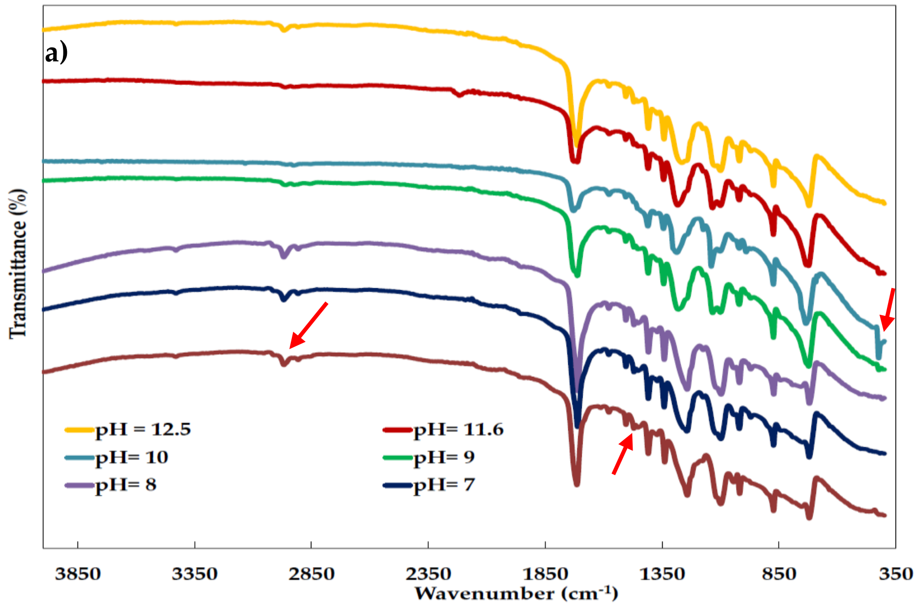

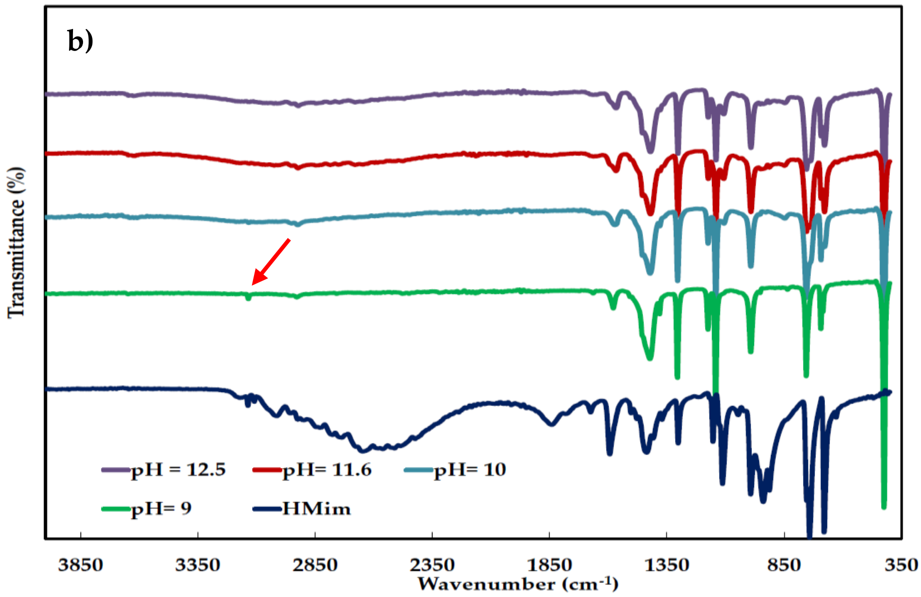

Fig. S28 FTIR spectrum of electrodeposited ZIF-67 a. films and b. powders at various solution pH at -0.8 V for 10 min.

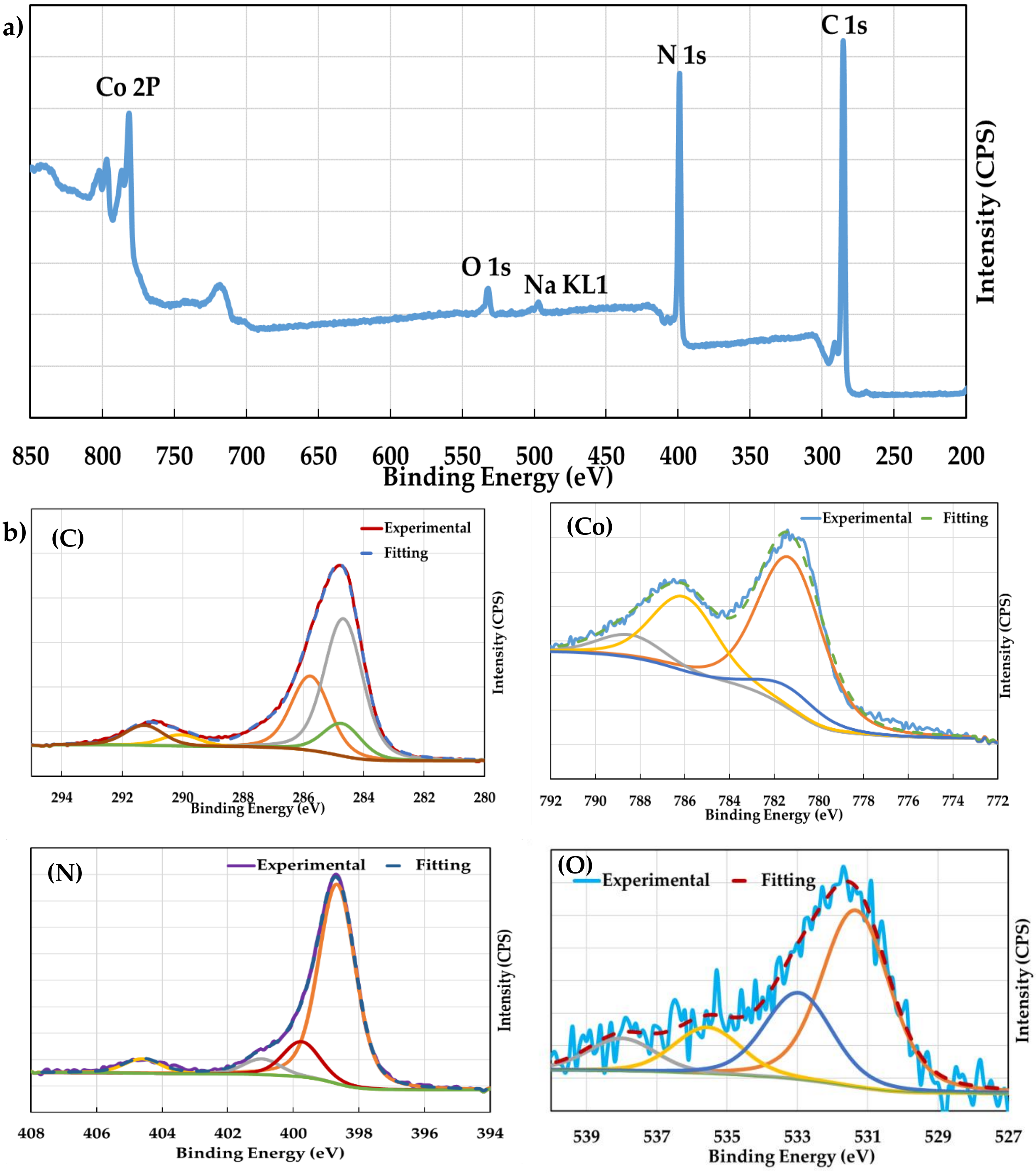
a)
Co 2P
O 1s
Na KL1
N 1s
C 1s
Intensity (CPS)
850 800 750 700 650 600 550 500 450 400 350 300 250 200
Binding Energy (eV)
b)
(C)
Experimental
Fitting
Intensity (CPS)
294 292 290 288 286 284 282 280
Binding Energy (eV)
(Co)
Experimental
Fitting
Intensity (CPS)
792 790 788 786 784 782 780 778 776 774 772
Binding Energy (eV)
(N)
Experimental
Fitting
Intensity (CPS)
408 406 404 402 400 398 396 394
Binding Energy (eV)
(O)
Experimental
Fitting
Intensity (CPS)
539 537 535 533 531 529 527
Binding Energy (eV)

Fig. S29 XPS survey spectrum (a. wide scan and d. high-resolution scans of Co, N, C and O) of ZIF-67 powder collected at reaction solution pH of 11.6 at -0.8 V for 10 min.

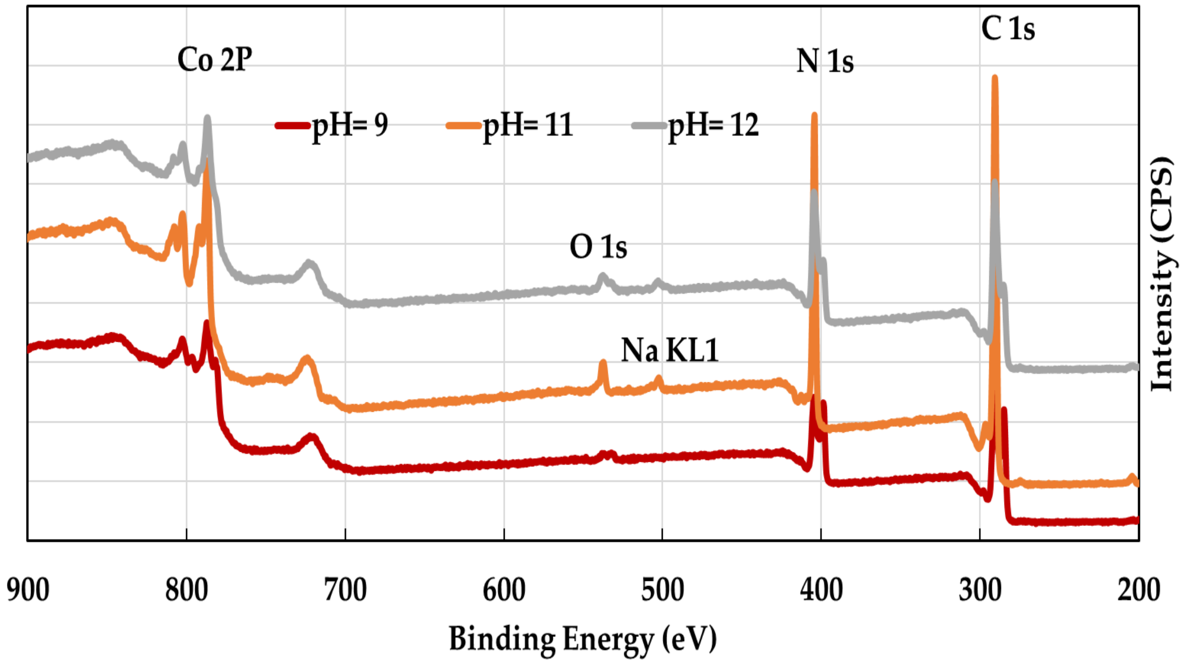

Fig. S30 Wide scan XPS survey spectra of ZIF-67 powders collected at various solution pH at -0.8 V for 10 min.

[1] A. Rovetta, Raiders of the lost correlation: a guide on using Pearson and Spearman coefficients to detect hidden correlations in medical sciences, Cureus 12(11) (2020).
[2] T. Dahiru, P-value, a true test of statistical significance? A cautionary note, Annals of Ibadan postgraduate medicine 6(1) (2008) 21-26.
[3] B. Kovač, I. Ljubić, A. Kivimäki, M. Coreno, I. Novak, Characterisation of the electronic structure of some stable nitroxyl radicals using variable energy photoelectron spectroscopy, Physical Chemistry Chemical Physics 16(22) (2014) 10734-10742.
[4] M. Meng, H. Yan, Y. Jiao, A. Wu, X. Zhang, R. Wang, C. Tian, A "1-methylimidazole-fixation" route to anchor small-sized nitrides on carbon supports as non-Pt catalysts for the hydrogen evolution reaction, RSC advances 6(35) (2016) 29303-29307.